

Neural Architecture and Locomotion

R.E.L. Turner*

Department of Mathematics

University of Wisconsin, Madison, Wisconsin 53706

e-mail: turner@math.wisc.edu

Received 23 September 2004

Abstract

Ascaris suum is a parasitic nematode that lives in pigs' intestines. It is a tempting subject for neurophysiologists in that it is 'simple', having only 300 neurons, about 80 of which are associated with locomotion. The muscular and neural structures are quite well understood, but the means by which they produce locomotion are not. In earlier work we developed a dynamic model for a single muscle cell; the model showed remarkably good correspondence with the voltage dynamics recorded in the laboratory. Here we use collections of model cells to represent dorsal and ventral muscle chains in the worm. The neuromuscular architecture in *Ascaris* is extremely complicated; we show, however, that by using suitable synaptic links between the model cells, we can create propagating waves of voltage variation that correspond to fictive motion.

1991 Mathematics Subject Classification. 37N25, 92C30.

Key words. Locomotion, muscle, neuron

1 Introduction

The nematode *Ascaris* has been studied for many decades (cf. [14] for references) as an example of a 'simple system' which, because of its size, enabled researchers to map its neural architecture. The interactions of the neural structure and the musculature have been well-studied by Stretton and collaborators [10] [2]. However, the means by which it carries out locomotion have not been understood. There

*The author acknowledges the hospitality of the Dipartimento di Matematica, Pisa, Italy.

have been studies of locomotion in several animals (Williams et al. [17]; Dale [1]; Grillner [3]; Tegnér and Grillner [11]. Some models start with a ganglion of cells as the fundamental unit, modeled as a single oscillator, while others start at the ionic level. The work of Dale [1] starts with a model of a neuron at the ionic level and is close in spirit to our approach. However, our basic building block is a model for a muscle cell rather than for a neuron as in [1]. As regards the controlling source for locomotion, the paper [18] is of particular interest in that it makes the point that neural connections alone or muscular connections alone provide a basis for crude locomotive patterns in the leech, though smoother patterns result from having both neural and muscular connections.

As a start on modeling the locomotion we explored a primitive model in [13]. A physiologically based model for a single muscle cell was developed in the paper [14] based on experimental data in the literature, recorded from single muscle cells in *Ascaris*. The principle sources were the papers of Martin and his collaborators [6] [7] [12].

While each muscle cell has a complicated morphology, we considered it to be isopotential for the model in [14] and continue with that assumption here. The data from the literature was used in [14] in a context similar to that used by Hodgkin and Huxley [4] in their classic paper on action potentials. Our model for a single muscle cell would correspond to the nonpropagating action potential in their framework.

In this paper we combine many copies of a muscle cell model in a model for a system representing the chains of muscle cells found along the body of *Ascaris*. There is a dorsal chain and a ventral chain with elaborate neuromuscular connections within each chain and between the two chains. We build a model with a simplified set of connections, complex enough to elicit propagating waves of contraction and relaxation, as occur in locomotion. It should be noted that Meade [8] found that when the head of *Ascaris* was ligatured, the worm produced a long lasting train of traveling waves of alternating contraction and relaxation. Our results are aimed at giving a rationale for such a periodic output.

2 A single muscle cell

Ascaris suum has approximately 50,000 muscle cells along its 30 cm. length and has 300 neurons, about 80 of which are involved in locomotion. For details on the neuro-muscular anatomy see [9], [10], [2] and their references). Each of the cells in our model will undergo timevarying oscillation in its potential, but there is no spatial variation of potential within a given muscle cell. The model in [14] was aimed at capturing the dynamic behavior seen in laboratory recordings from muscle cells (cf. [16] and other papers listed in [14]).

We briefly recall the components that made up the original muscle cell model; see [14] for more details. The principle cation involved in the depolarization of a muscle cell is calcium (cf. Weisblat and Russell [16] and Martin et al [6]). Hyperpolarization is achieved through three principle types of currents. Two are potassium currents: a non-inactivating potassium current of Hodgkin-Huxley type and a potas-

sium current of type A (Martin et al [6]). A third source of hyperpolarization is a calcium activated chloride current (Thorn and Martin [12]) and in the model it is essential for the termination of the trains of spikes. Finally, there is a leak current based on (Martin et al [6]).

The calcium current across the cell membrane of a model muscle cell is taken to be:

$$I_{Ca} = g_{Ca} \cdot e^2 \cdot f \cdot (V - V_{Ca}).$$

Here g_{Ca} is the maximum calcium conductance for the cell in micro-Siemens; e is a unitless activation parameter; f is an inactivation parameter; V is the cytoplasmic voltage in millivolts (relative to an extracellular voltage of zero); and V_{Ca} is the calcium reversal potential in millivolts. Values of the parameters used are given in the Appendix. The dynamics of the gating variables e and f are described using the standard Boltzmann type rate functions, assuming each 'gate' has just two states: closed and open. For activation these correspond to $e = 0$ and $e = 1$, respectively.

For the e-gate the transition probabilities of a passage from closed to open and from open to closed, respectively, are taken as:

$$a_e(V) = \exp((V - v_{ae})/s_{ae}), \quad b_e(V) = \exp((V - v_{be})/s_{be})$$

where V is the voltage in the interior of the cell, and v_{ae} , s_{ae} , v_{be} , s_{be} ('e' referring to the 'e' gate, etc.) are parameters given in the Appendix. These produce the equilibrium state and time 'constant',

$$e_\infty(V) = \frac{a_e(V)}{a_e(V) + b_e(V)}, \quad \tau_e(V) = \frac{1}{a_e(V) + b_e(V)},$$

respectively, (cf. Hodgkin and Huxley [4]). The dynamics for e are then given by

$$\frac{de}{dt} = \frac{e_\infty(V) - e}{\tau_e(V)}.$$

so that the gating variable e is being driven toward the 'equilibrium' $e_\infty(V)$ with a time parameter $\tau_e(V)$, both quantities varying with the potential V . In fact, we speed up the e gate by including a factor $\sigma = 2.1$ (cf equation 5.2). In a completely analogous fashion one describes the dynamics for the gating variable f using parameters v_{af} , s_{af} , v_{bf} , s_{bf} and, again, we include a factor σ in equation (5.3). These are among several changes made in the parameters from [14]. Such changes do not alter the basic characteristics of the voltage output (cf. Figure 1), but do change the number of spikes in a burst and the time scales involved. In [14] we were aiming to duplicate the recording in [16] in which there were three spikes per burst. However Weisblat observed from three to eight spikes and the present model gives six as seen in Figure 1.

The 'non-inactivating' potassium current is given by

$$I_K = g_K \cdot n \cdot m \cdot (V - V_K),$$

the terms being similar to those in the calcium current. The activation parameter is n and m is responsible for a slow inactivation. Moreover, we replace the Boltzmann

relaxation times to constants (cf. Appendix). A rapidly inactivating potassium current, I_A , is described by:

$$I_A = g_A \cdot p^4 \cdot q \cdot (V - V_K),$$

The activation parameter being p , and the inactivation parameter, q . Again, as for the calcium current, the parameters for the potassium currents were chosen to approximate the results of Martin [6]. The leak current was taken to be

$$I_L = g_L \cdot (V - V_L)$$

with the parameters obtained from Martin et al [6].

The work of Thorn and Martin [12] was dedicated to studying a calcium dependent chloride channel in the muscle cell. The mechanics of activation of the chloride channels by calcium are not discussed in [12] and so we incorporated a mechanism which allows for some accumulation of calcium and a subsequent opening of chloride channels when a threshold level of calcium is reached. We took into account the time lag (from 2 to 3 seconds, cf. [12], p. 44) between the appearance of calcium and the opening of the chloride channels. Not knowing the mechanism, we introduced a discrete version of a diffusion. We considered a fraction, r , of the total calcium influx (described above) to be the pool acting on the chloride channels. Letting a_0 denote the level of the calcium in the segregated pool, the discrete diffusion takes place over hypothetical 'sites' having calcium levels a_0, a_1, a_2, a_3 (equations 5.8-5.11). The concentration of calcium a_2 is allowed to rise to a threshold and subsequently control the gating of the chloride channels through a parameter b satisfying $0 \leq b \leq 1$. The current has the form

$$I_{Cl} = g_{Cl} \cdot b \cdot (V - V_{Cl}).$$

The mechanism allows for some time delay in the action of the entering calcium and has some smoothing effect on the calcium level, an effect that would occur during diffusion. We also include a buffering of calcium with constant k .

Combining the components just described, we obtain the equations governing a single model cell. Its state is described by the variables (V, e, f, n, m, q, b) , and calcium concentrations $a_i, i = 0, 1, 2, 3$. The full equations are given in the Appendix. Equation (5.1), below, is a current balance, (5.2) through (5.7) control gating kinetics, and (5.8) through (5.11) describe the diffusive approximation for calcium.

For use in this paper we will abbreviate the full set of equation using V for the membrane voltage and $G = (e, f, n, m, q, b, a_0, a_1, a_2, a_3)$ to denote the combined gating and diffusion variables. With this notation each muscle cell is then governed by a system of equations (for capacitance c_m cf. (5.15)

$$c_m \frac{dV}{dt} = I(V, G) \tag{2.1}$$

$$\frac{dG}{dt} = F(V, G) \tag{2.2}$$

where $I(V, G)$ stands for the sum of currents on the right hand side of equation (5.1) in the Appendix and $F(V, G)$ stands for the right hand sides of equations (5.2) through (5.11) in that collection.

With variation in the calcium segregation parameter r the model produces trains of 2 to 8 spikes, a *burst*, alternating with quiescent intervals of about 900 milliseconds during which the potential was around the equilibrium value of -33 millivolts. In the model for a single cell the alternation continues unabated. In the behaving animal the alternating bursts and troughs last from 7 to 20 seconds and constitute a *bout*. We shall see that the bouts will arise from the linkages in the more complex system. In Figure 1 we show the output of the cell model during an interval of 6 seconds. In [14] Figure 3 one can see that the cell model from that paper gives a very good approximation to the recorded muscle cell behavior on the two fastest time scales.

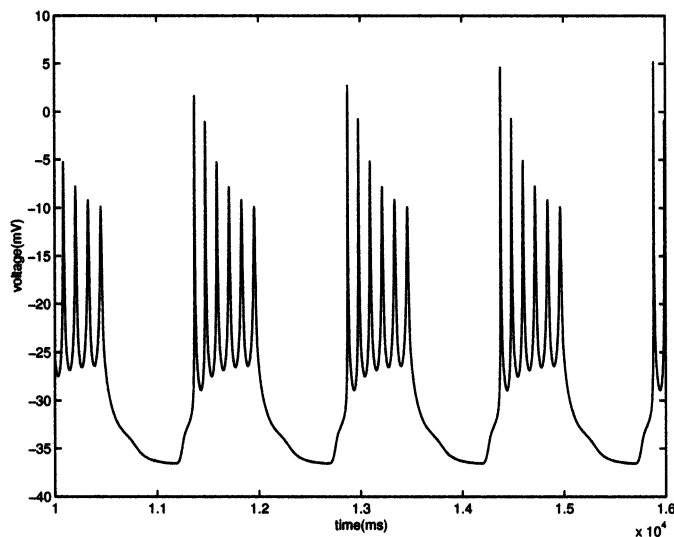


Figure 1. Bursts from the model during a 6 second interval

3 Chains of muscle cells

The model proposed in this paper uses eight dorsal-ventral pairs of muscle cells, each being the type described in the previous section. They have voltages: (V_{2k-1}, V_{2k}) , $k = 1, 2, \dots, 6, 7, 8$. The quantities V_1, V_3, \dots denote the voltages of the dorsal cells and V_2, V_4, \dots those of the ventral cells (cf Figure 2). The linkages among the cells will be of three types: self linkage due to stretch, reciprocal linkage between each dorsal-ventral pair, and lateral linkages.

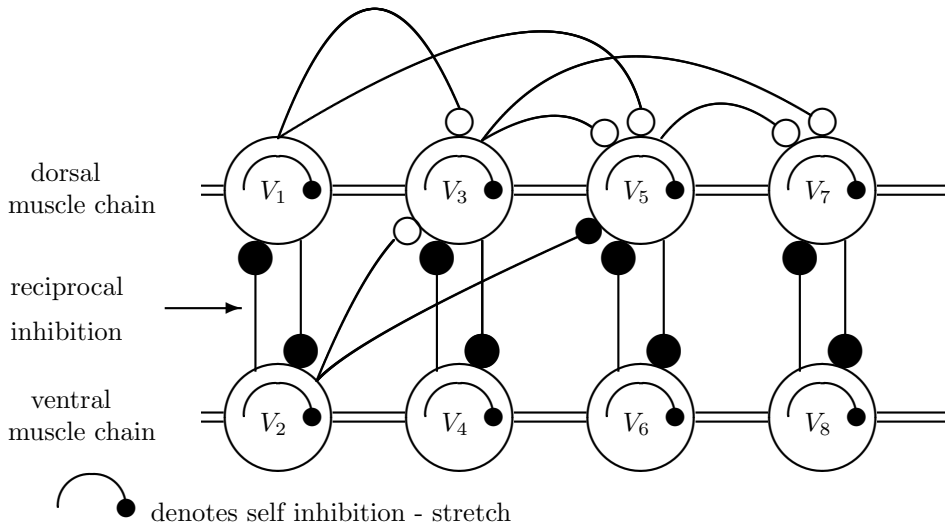


Figure 2. Schematic showing a portion of the chains of twinned dorsal and ventral cells. The dark circles indicate an inhibitory influence and the open circles, an excitatory influence.

Stretch:

In the model each cell is given some self-inhibition (cf. Figure 2) to correspond to the effect of stretch receptors. Clear data on stretch receptors is lacking, but the evidence for their existence is compelling (cf. the remarks in the intro to [14]). What we have included is a mechanism to have a negative input current to a cell when the amplitude of its voltage rises. This is done via the quantity \tilde{V} generated from the equations for the cell itself (cf. (5.20)). The equations result in a 'smoothed' voltage \tilde{V} which rises with the onset of a train of bursts (lasting a second or two), brings the bout to an end, and subsides near the end of the bout (the reciprocal inhibition will also aid in suppressing a bout). A current $g_S \cdot \tilde{V}$ is subtracted from the right hand side of the current equation for a cell to represent the effect of 'stretch'. The quantity \tilde{V} is designed to be positive (cf. Figure 3) and so with a positive conductance g_S , one has 'self-inhibition'.

Reciprocal Inhibition:

Further, in the model, each dorsal-ventral twinned pair (cf. Figure 2) with voltages (V_{2k-1}, V_{2k}) is equipped with reciprocal inhibition. This is well documented ([10], [2]) though the mechanism for this inhibition in our model is considerably simplified. Rather than have an indirect inhibition between muscle cells, achieved through a neuromuscular structure, we realize it in a direct way.

To describe the reciprocal linkage among cells, we denote any one of the cell voltages (dorsal or ventral) by V and denote the voltage of its 'twin' by W . The

equations include a smoothing mechanism to create a quantity \tilde{W} from W (cf. (5.21)). As above, the quantity \tilde{W} is positive (cf. Figure 3) and the reciprocal inhibition is effected through a term $g_R \cdot \tilde{W}$, with $g_R > 0$, subtracted from the right hand side of the current equation (2.1).

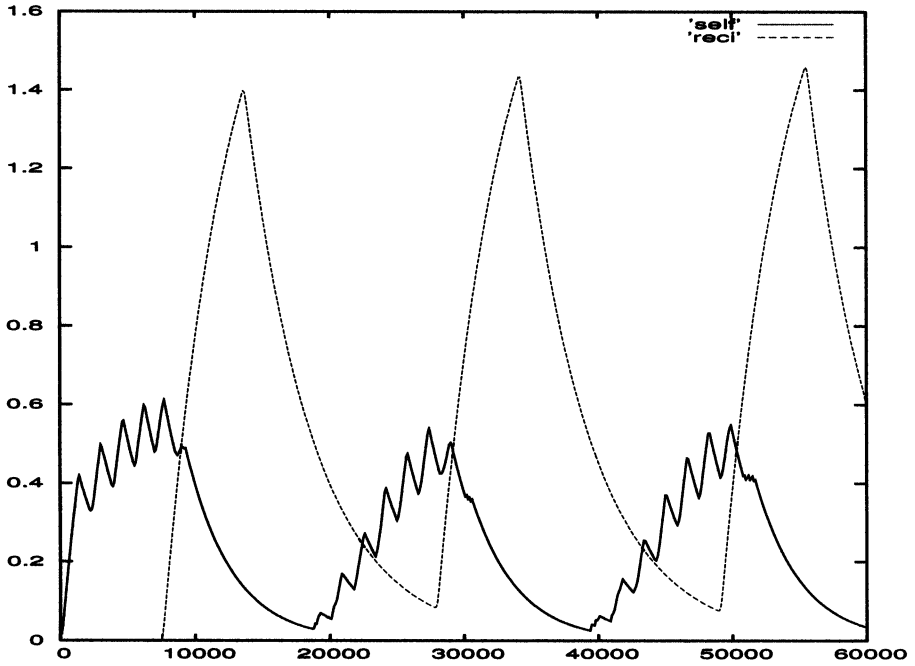


Figure 3. A graph with abscissa in milliseconds and ordinate showing the self inhibitory input \tilde{V} (solid) and reciprocal input \tilde{W} (dashed).

From (2.1) and (2.2) we then obtain an intermediate set of equations for the voltages in the separate muscle cell pairs:

$$c_m \frac{dV_i}{dt} = I(V_i, G_i) - g_S \cdot \tilde{V}_i - g_R \cdot \tilde{W}_i \tag{3.1}$$

$$\frac{dG_i}{dt} = F(V_i, G_i) \tag{3.2}$$

$$c_m \frac{dV_{i+1}}{dt} = I(V_{i+1}, G_{i+1}) - g_S \cdot \tilde{V}_{i+1} - g_R \cdot \tilde{W}_{i+1} \tag{3.3}$$

$$\frac{dG_{i+1}}{dt} = F(V_{i+1}, G_{i+1}), \text{ for } i = 1, 3, 5, 7, 9, 11, 13, 15 \tag{3.4}$$

where g_S is a 'stretch' conductance, and g_R is a 'reciprocal' conductance (see the Appendix for numerical values). We note again that the two added currents for each cell are hyperpolarizing; that is, they drive the voltage toward more negative

values. This completes the description as far as single twinned pairs is concerned. We repeat that for i an odd integer \tilde{W}_i is a smoothed version of V_{i+1} and \tilde{W}_{i+1} is a smoothed version of V_i

Lateral Linkage:

The linkage between pairs will ultimately be responsible for the delays between the voltage excursions at individual sites and thus the fictive locomotion. We repeat at this point that the model does not attempt to capture the intricacies of all the neural-muscular interactions (it is so complicated that one cannot successfully isolate the components in the laboratory to carry out desired experiments). We have, frankly, experimented with a variety of linkages (as evolution may have done) to achieve a collection of time dependent voltages in the various muscle cells. A well accepted tenet of muscle physiology is that a depolarization (excursion toward more positive values of voltage) in a muscle cell induces contraction in the cell and a hyperpolarization (excursion toward more negative values) induces relaxation. It is in this sense that the voltages achieved in our model produce waves of contraction and relaxation that accompany locomotion in the behaving worm. It should be noted that there are gap-junction linkages between muscle cells in *Ascaris*. However, as in [14], we exclude them from consideration for long term dynamics, assuming that the influx of calcium has effected a closing of these junctions [15].

The linkage among the cells for the dorsal-ventral 'twins' is identical for all pairs, while the lateral linkages vary with the cell. More specifically the lateral linkages are achieved through a function

$$\text{syn}(i, j) = \tanh(V'_j - 0.3) * (V_i - V_r)$$

where V'_j is a smoothed version of the voltage V_j in the presynaptic cell (V'_j corresponds to s_2 in equation (5.17)) and $V_r = -38mV$ is a reversal potential for the channel affecting the postsynaptic signaling. That is, a channel in the postsynaptic cell which tries to drive the potential of that cell towards -38 mV.

A strength $a(i, j)$ is further associated with the cell 'j' to cell 'i' coupling. The final form of the linkage from the presynaptic cell j to the postsynaptic cell i includes a tanh to limit the size of the signal for certain sites. The final form is:

$$L(i, j) = a(i, j) \cdot \text{syn}(i, j) \tag{3.5}$$

except for adjacent odd numbered cells (links 1 to 3, 5 to 7, etc) in which case it is:

$$L(i, j) = \tanh(a(i, j) \cdot \text{syn}(i, j)). \tag{3.6}$$

The strengths in the system were taken to be (positive \approx excitatory):

- a(1,3) = 6.0, a(2,3) = 1.5
- a(3,5) = 30.0, a(1,5) = 15.0, a(2,5) = -15.0
- a(5,7) = 30.0, a(3,7) = 15.0, a(2,7) = -15.0
- a(7,9) = 30.0, a(5,9) = 15.0, a(3,9) = -15.0
- a(9,11) = 30.0, a(7,11) = 15.0, a(5,11) = -15.0
- a(11,13) = 30.0
- a(13,15) = 30.0

with all other $a(i, j) = 0$. The linkage input to cell i is thus the sum:

$$L(i) = \sum_j L(i, j). \tag{3.7}$$

We note again that the linkages given are much sparser than those in the worm, but serve to illustrate the possibility that the architecture can produce the waves.

The final system, in concise form (see Appendix for more detail) is:

$$c_m \frac{dV_i}{dt} = I(V_i, G_i) - g_S \cdot \tilde{V}_i - g_R \cdot \tilde{W}_i + L(i) \tag{3.8}$$

$$\frac{dG_i}{dt} = F(V_i, G_i) \tag{3.9}$$

$$c_m \frac{dV_{i+1}}{dt} = I(V_{i+1}, G_{i+1}) - g_S \cdot \tilde{V}_{i+1} - g_R \cdot \tilde{W}_{i+1} + L(i+1) \tag{3.10}$$

$$\frac{dG_{i+1}}{dt} = F(V_{i+1}, G_{i+1}), \text{ for } i = 1, 3, 5, 7, 9, 11, 13, 15. \tag{3.11}$$

4 Computation

The equations in the system (3.8-3.11) were solved using a differential equation solver 'dvide' from Lawrence Livermore National Laboratory, Berkeley, California. It was used in the Method Flag mode 22 for a stiff equation and so generated variable step sizes. The reported data was generated using tolerances $ATOL = RTOL = 10^{-7}$.

In our simulations each single cell starts with initial data: $V = -30$ mV , $f = 1.0$, $q = 1.0$, $m = 1.0$. All of the remaining variables start at zero. We note, however, that the numerical simulation was run for an extended time (up to 360 seconds of model time) and the output below is taken from the period 300 to 360 seconds when the solution appeared to have reached a periodic state. We do not address the initial behavior starting from rest. Further, a slight difference in the dorsal and ventral model equations was included for each pair in the first 20 seconds so as to break the symmetry in the pairs.

The passage from the output of voltages to a fictive locomotion is done by choosing an adhoc way of translating the individual voltage excursions into amplitudes of contraction and relaxation. Given the large number of muscle cells and the dispersed nature of the inputs from neurons to cells, it is extremely difficult to make a cogent choice for the model. We have chosen to interpret the bursts in a cell as initiating a contraction that grows during the bout and subsides toward the end of the bout. While we also do some subsequent processing of the output signal we have incorporated a pair of equations that transform the voltage output of each cell into a signal that rises with a bout and then subsides at the end of the bout. This output \tilde{V} is generated via the equations

$$\frac{dR}{dt} = 0.02 [\text{sig}(-28, 0.5, V) - R]/\text{sig}(0.4, .05, R) \tag{4.1}$$

MATLAB and these curves were used as frames for a movie in MATLAB. Figure 5 shows the state of the chain of cells at three successive times, frames 8,12,16, out of 30.

A positive amplitude corresponds to a dorsal contraction and ventral relaxation, while a negative amplitude corresponds to the reverse. Thus, while the progressing waves of contraction relaxation are captured in the simulation, in regard to the physical shape of the worm, a dorsal contraction means a bend which is convex upward and a ventral contraction induces a bend which is concave downward. Hence the curves in Figure 5 should be inverted in the axis of zero amplitude to give an indication of the shape of the worm.

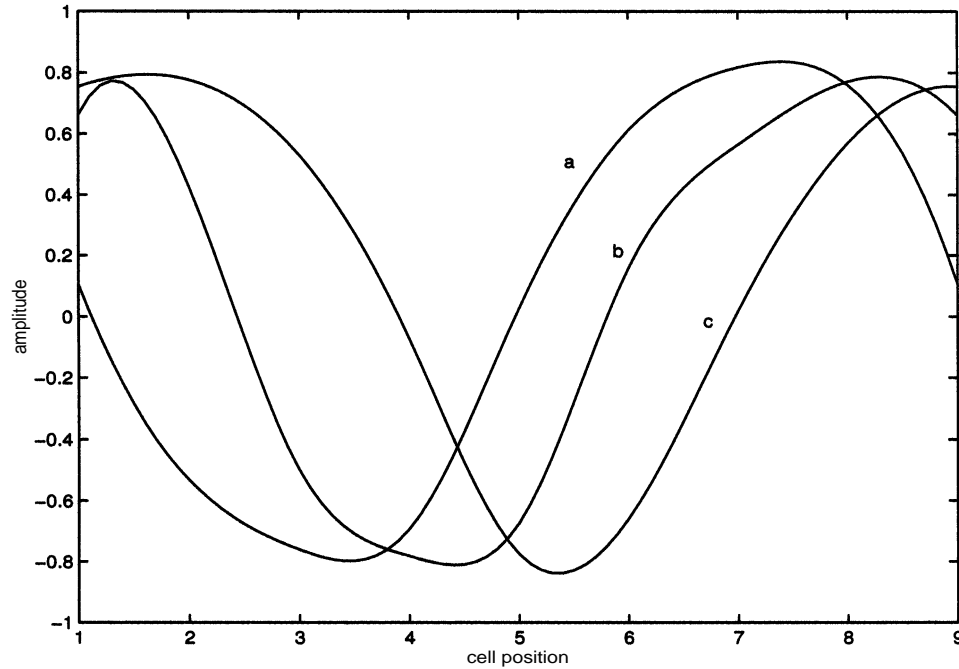


Figure 5. Frames from 'movie', a=frame 6, b=frame 12, c=frame 18

As noted in the introduction, Meade [8] observed long lasting train of traveling waves of alternating contraction and relaxation. Our results do capture such behavior; the successive crests and troughs move to the right as time progresses.

5 Appendix

The equations for a single muscle cell are:

$$c_m \frac{dV}{dt} = - [g_{Ca} e^2 \cdot f \cdot (V - V_{Ca}) + g_{Kn} \cdot m \cdot (V - V_K) + g_L \cdot (V - V_L)]$$

$$\frac{d\hat{V}}{dt} = 0.7 [\text{sig}(0.2, 0.1, R) - 0.1192 - \hat{V}] / \text{sig}(0.3, .02, \hat{V}). \quad (4.2)$$

We call the voltage \hat{V} the transform of V . Using V for the voltage of a dorsal cell, and W for the voltage of its ventral 'twin', we first show a plot of the difference in transforms. At a given location along the worm, a positive amplitude for \hat{V} and a negative amplitude for \hat{W} would correspond to the dorsal part of that section being in contraction and its ventral (opposing side) being in relaxation. Thus a positive sign for $\hat{V} - \hat{W}$ we take as inducing a curvature of the worm, convex upward. Likewise a negative amplitude for $\hat{V} - \hat{W}$ would induce a curvature concave downward. The Figure 4 shows a plot of $\hat{V} - \hat{W}$ versus time for the first pair of cells (V_1, V_2).

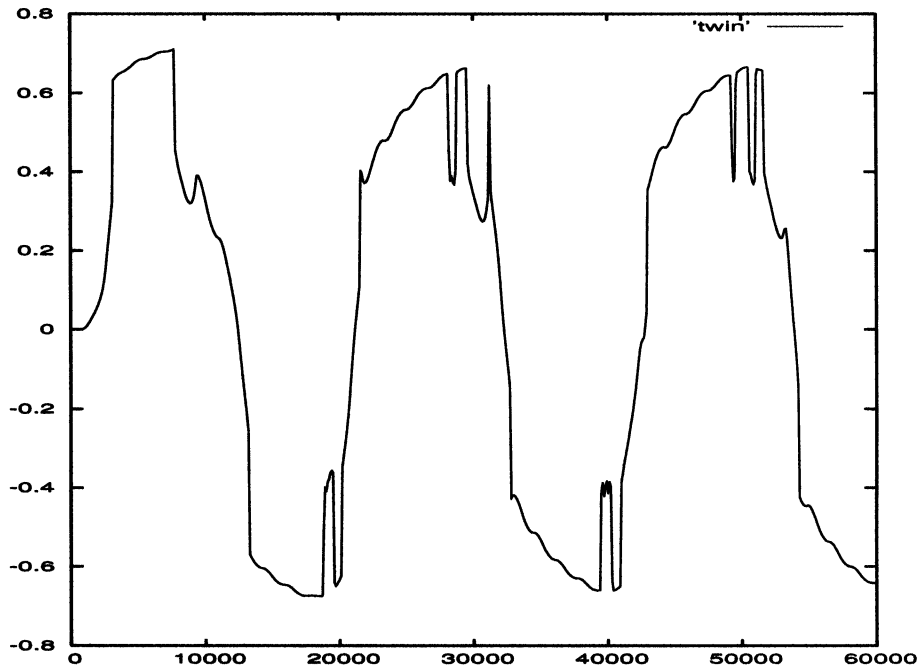


Figure 4. The dorsal output minus the ventral output (after processing) for the first pair of cells, abscissa in $\text{ms } 10^{-1}$.

We take the eight dorsal-ventral twins as situated at equidistant sites along a hypothetical worm. Using a ninth twinned pair identical to the first one we have amplitudes of $\hat{V} - \hat{W}$ at sites 1,2,...9. The output $\hat{V} - \hat{W}$ for each pair is further processed. We read the values every 50 milliseconds during the period from 300 to 360 seconds. This data set of 1200 entries is averaged in groups of 50: items 1 to 50, 5 to 55, etc to produce a data set of size 114. These amplitudes at the nine sites, a jagged plot, were converted to a smooth curve using the Bezier splines in

$$+g_A \cdot p^4(V) \cdot q \cdot (V - V_K) + g_{Cl} \cdot b \cdot (V - V_{Cl}) \quad (5.1)$$

$$\frac{de}{dt} = \frac{e_\infty(V) - e}{\tau_e(V)} \cdot \sigma \quad (5.2)$$

$$\frac{df}{dt} = \frac{f_\infty(V) - f}{\tau_f(V)} \cdot \sigma \quad (5.3)$$

$$\frac{dn}{dt} = \frac{n_\infty(V) - n}{\tau_n} \quad (5.4)$$

$$\frac{dm}{dt} = \frac{m_\infty(V) - m}{\tau_m} \quad (5.5)$$

$$\frac{dq}{dt} = \frac{q_\infty(V) - q}{\tau_q} \quad (5.6)$$

$$\frac{db}{dt} = \frac{b_\infty(a_2) - b}{\tau_b} \quad (5.7)$$

$$\frac{da_0}{dt} = -rI_{Ca} - 2ka_0 \quad (5.8)$$

$$\frac{da_1}{dt} = \delta(a_2 - 2a_1 + a_0) - ka_1 \quad (5.9)$$

$$\frac{da_2}{dt} = \delta(a_3 - 2a_2 + a_1) - ka_2 \quad (5.10)$$

$$\frac{da_3}{dt} = \delta(-2a_3 + a_2) - ka_3 \quad (5.11)$$

$$\begin{array}{ll} v_{ae} = -27.0 \text{ mV} & v_{bn} = 25.0 \text{ mV} \\ s_{ae} = 8.0 \text{ mV} & s_{bn} = -8.0 \text{ mV} \\ v_{be} = 191.0 \text{ mV} & v_{am} = 57.0 \text{ mV} \\ s_{be} = -59.0 \text{ mV} & s_{am} = -36.0 \text{ mV} \\ v_{af} = -25.0 \text{ mV} & v_{bm} = -28.0 \text{ mV} \\ s_{af} = -2.5 \text{ mV} & s_{bm} = 38.0 \text{ mV} \\ v_{bf} = -31.0 \text{ mV} & v_{aq} = -33.0 \text{ mV} \\ s_{bf} = 5.0 \text{ mV} & s_{aq} = -4.0 \text{ mV} \\ v_{an} = -45.0 \text{ mV} & v_{bq} = -27.0 \text{ mV} \\ s_{an} = 8.0 \text{ mV} & s_{bq} = 4.0 \text{ mV} \end{array} \quad (5.12)$$

though the Boltzmann relaxation times for the n, m, q gates are replaced by the constants: $\tau_n \equiv 10$ ms, $\tau_m \equiv 476$ ms, $\tau_q \equiv 24$ ms, respectively.

We make repeated use of the sigmoidal function:

$$\text{sig}(r, s, v) = \frac{1}{1 + \exp(\frac{r-v}{s})}. \quad (5.13)$$

The activation gate for the current I_A is taken to be $p_\infty(V) = \text{sig}(v_{ap}, s_{ap}, v)$, with $v_{ap} = -34$ mV, and $s_{ap} = 0.8$ mV. The gating for the chloride current uses the 'calcium level' a_2 via the sigmoidal function

$$b_\infty(a_2) = \text{sig}(1.0, .005, \frac{a_2}{a}) \tag{5.14}$$

with activation level $a = .007$ and $\tau_b = 143ms$.

Conductances in microSiemens, reversal potentials, and other parameters are:

$g_{Ca} = 3920.0 \mu S$	$g_{Cl} = 2.9 \mu S$
$g_A = 2.1 \mu S$	$g_K = 3.5 \mu S$
$g_S = 35 \mu S$	$g_R = 40 \mu S$
$g_L = 6.0 \mu S$	$v_{Ca} = 50.0 mV$
$v_{Cl} = -55.0 mV$	$v_K = -50.0 mV$
$v_L = -30.0 mV$	$k = 1.18 s^{-1}$
$c_m = 0.01 \mu F$	$r = 0.0011$
$\delta = 1.47 s^{-1}$	$\sigma = 2.1$

This completes the list of parameters for the single muscle cell model.

Next we describe the elements used in the system model. For the stretch effect we use the threshold function (5.13) with a discrete diffusion and use s_6 below to generate the smoothed function \tilde{V}

$$\frac{ds_1}{dt} = 0.4 \text{sig}(1, 0, .02, V + 31) - 0.2s_1 \tag{5.16}$$

$$\frac{ds_2}{dt} = 0.42(s_1 - s_2) \tag{5.17}$$

$$\frac{ds_3}{dt} = 2.1 \text{sig}(0.6, .005, s_2) + .84(s_4 - 2s_3) - 2.352s_3 \tag{5.18}$$

$$\frac{ds_k}{dt} = .84(s_{k+1} - 2s_k + s_{k-1}) - 2.352s_3, \quad k = 4, 5, \dots, 10 \tag{5.19}$$

$$\frac{d\tilde{V}}{dt} = .4 \text{sig}(.003, .0002, s_6) - 0.2\tilde{V} \tag{5.20}$$

with $s_{11} \equiv 0$.

Letting W be the voltage 'twin' of V , we generate \tilde{W} , effecting the reciprocal inhibition, using:

$$\frac{d\tilde{W}}{dt} = 0.4 \text{sig}(1.0, .02, W + 29) - 0.3\tilde{W}. \tag{5.21}$$

References

- [1] T. R. Dale, *Experimentally derived model for the locomotor pattern generator in the Xenopus embryo*, Journal of Physiology **492.2** (1995), 473-488, 489-510.

- [2] R. E. Davis, & A. O. W. Stretton, *The motornervous system of Ascaris: electrophysiology and anatomy of the neurons and their control by neuromodulators*, Parasitology **113** (1996), S97-S117.
- [3] S. Grillner, *Bridging the gap - from ion channels to networks and behavior*, Current Opinion in Neurobiology **9**(6)(1999), 663-669.
- [4] A. L. Hodgkin & A. F. Huxley, *A quantitative description of membrane current and its application to conduction and excitation in nerve*, Journal of Physiology **117**(1952), 500-544.
- [5] M. Jarman (1959), *Electrical activity in the muscle cells of Ascaris lumbricoides*. Nature **184** (1959), 1244.
- [6] R. J. Martin, P. Thorn, P., K. A. F. Gration, & I. D. Harrow, *Voltage-activated currents in somatic muscle of the nematode parasitic Ascaris suum*. Journal of Experimental Biology **173**(1992), 75-90.
- [7] R. J. Martin & M. A. Valkanov, M. A. (1996), *Effects of acetylcholine on a slow voltage-activated non-selective cation current mediated by non-nicotinic receptors on isolated Ascaris muscle bags*, Experimental Physiology **81** (1996), 909-925.
- [8] J. A. Meade, *Intracellular recordings from neurons and muscle cells in a semi-intact preparation of the nematode Ascaris suum: Implications for Ascaris locomotion*, Thesis, University of Wisconsin, Madison (1991).
- [9] A. O. W. Stretton, A. O. W. (1976), *Anatomy and development of the somatic musculature of the nematode Ascaris*, Journal of Experimental Biology **64** (1976), 773-788.
- [10] A. O. W. Stretton, R. E. Davis, J. D. Angstadt, J. E. Donmoyer, & C. D. Johnson, *Neural control of behaviour in Ascaris*, Trends in Neuroscience **8**(1985), 294-300.
- [11] J. Tegnér & S. Grillner, *Interactive effects of the GABA_Bergic modulation of calcium channels and calcium-dependent potassium channels in lamprey*, Journal of Neurophysiology **81** (1999), 1318-1329.
- [12] P. Thorn & R. J. Martin, *A high-conductance calcium-dependent chloride channel in Ascaris suum muscle*, Quarterly Journal of Experimental Physiology **73**(1987), 31-49.
- [13] R. E. L. Turner, *Phase setting and Locomotion*, Computational Neuroscience, Trends in Research. ed. Bower, J., 873-877. Plenum, New York, 1997.
- [14] R. E. L. Turner, *A model for an Ascaris muscle cell*, Experimental Physiology, **86.5** (2001), 551-559.
- [15] A. Warner, *The gap junction*, Journal of Cell Science **89** (1988), 1-7.
- [16] D. A. Weisblat & R. L. Russell, *Propagation of electrical activity in the nerve cord and muscle syncytium of the nematode Ascaris lumbricoides*, Journal of Comparative Physiology **107** (1976), 293-307.
- [17] T. L. Williams, K. A. Sigvardt, N. Kopell, G. B. Ermentrout, & M. Remler, *Forcing of coupled nonlinear oscillators: studies of intersegmental coordination in the lamprey central pattern generator*, Journal of Neurophysiology **64** (1990), 862-871.
- [18] X. Yu, B. Nguyen, & W. O. Friesen, *Sensory feedback can coordinate the swimming activity of the leech*, The Journal of Neuroscience **19**(11) (1999), 4634-4643.